

against smaller disturbances to make it possible to do very precise experiments inside an average laboratory room during the daytime when other activities are in progress. This is an immense gain over the situation encountered when there is no shielding.

ACKNOWLEDGMENTS

The original motivation for building the shielded solenoid grew out of conversations with Professor Daniel Kleppner.

He found in work on the hydrogen maser that shields could be used to produce a region free from disturbance by external fields. The success of the solenoid was due in part to the very careful machining and winding which was performed by Stanley Gardner. Jack Sanderson played a major role in writing the FORTRAN program for computing the magnetic field in the shielded solenoid. We are indebted to Chris Balling for making the optical pumping measurements.

"Floating Wire" Technique for Testing Magnetic Lenses

URIEL VOGEL*

Cyclotron Laboratory, Department of Physics, The University of Michigan, Ann Arbor, Michigan

(Received 6 October 1964; and in final form, 19 October 1964)

Improvements in the well-known technique of using a current-carrying wire to simulate particle trajectories in a magnetic field are described. As presently used, the parameters of magnetic lenses can be determined for a resolution in momentum as large as 10^4 .

I. INTRODUCTION

THE ion-optical system associated with The University of Michigan 83-in. cyclotron¹ is designed to provide a resolution in momentum of $p/\Delta p \approx 2 \times 10^4$. Various techniques were used in the testing and the alignment of the system of magnets, one of which was the familiar "floating-wire" technique.^{2,3}

The limitations on the accuracy of the technique are set by (1) the accuracy with which the wire position can be determined, (2) the stability of the magnetic field and the current in the wire, and (3) the friction and hysteresis of the pulley bearings and the wire, respectively.

The purpose of this paper is to describe the methods used for minimizing these limitations.

II. THE "FLOATING-WIRE" TECHNIQUE

The technique is based on the equivalence of the equations governing the position of equilibrium of a flexible wire carrying an electric current in a magnetic field, and the trajectory of a charged particle passing through the same magnetic field.

For a wire, we have³

$$\mathbf{n}/\rho = (\mathbf{t} \times \mathbf{B}) \cdot i/T + m\mathbf{g}/T, \quad (1)$$

* Present address: Space Physics Research Laboratory, The University of Michigan, Ann Arbor, Michigan.

¹ J. Bardwick, J. M. Lambert, and W. C. Parkinson, Nucl. Instr. Methods **18**, 19, 105 (1962).

² D. R. Bach, W. J. Childs, R. W. Hockney, P. V. C. Hough, and W. C. Parkinson, Rev. Sci. Instr. **27**, 516 (1956).

³ "Use of Wire Loop in Locating the Orbital Surface of a Cyclotron Field," G. R. Lamberton, UCRL-3366.

and for particles³

$$\mathbf{n}/\rho = (-\mathbf{t} \times \mathbf{B}) \cdot e/p, \quad (2)$$

where ρ is the radius of curvature of the trajectory, \mathbf{n} is the unit vector in the direction of radius of curvature of the trajectory, \mathbf{t} is the unit vector tangential to the trajectory, \mathbf{B} is the magnetic field, T is the tension in wire, e is the charge of particle, p is the momentum of particle, i is the electric current in the wire, and $m\mathbf{g}$ is the weight of a unit length of the wire.

Assuming the wire to lie in a horizontal plane, the factor $m\mathbf{g}$ can be ignored, and the resulting radii of curvature ρ will be equal provided

$$i/T = -e/p. \quad (3)$$

The wire will then align itself in a position of equilibrium identical with the trajectory of the particle.

The absolute value of the momentum p of a particle remains constant throughout its passage in the magnetic field so that, for the equivalence to hold, it is necessary to keep i/T constant.

The experimental arrangement is shown schematically in Fig. 1. The "floating wire" (I) is anchored at one side of the magnet, the other end being stretched over a pulley and kept under tension T by a weight G .⁴ In equilibrium, position (I) is equivalent to a particle ray of a certain momentum. To find the image point of the magnetic lens,

⁴ The problem is considerably simplified when the magnets can be mounted vertically and the tension applied to the wire without using a pulley. This was not feasible for these magnets.

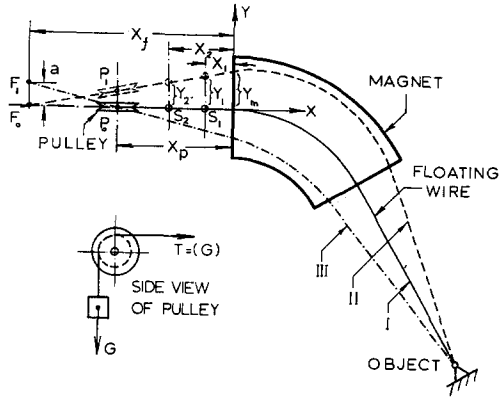


FIG. 1. Schematic of "floating-wire" experimental setup.

the position of the wire is measured at two points, X_1 and X_2 inches from the face of the magnet poles. The pulley is then shifted and the wire permitted to reach a new position of equilibrium (II). The new positions are measured at the same distances X_1 and X_2 from the face of the magnet and the shifts y_1 and y_2 (in the y direction) determined. Since i and T were held constant, the rays (I) and (II) correspond to the same momentum and their intersection, therefore, determines the image point. The distance X_f of the image from the face of the magnet is given by

$$X_f = (X_2 y_1 - X_1 y_2) / (y_1 - y_2). \quad (4)$$

The accuracy with which X_f can be determined now follows by differentiation:

$$\Delta X_f = (-X_2 y_2 \Delta y_1 + X_1 y_1 \Delta y_2) / (y_1 - y_2)^2, \quad (5)$$

where ΔX_f , Δy_1 , and Δy_2 are the errors in X_f , y_1 , and y_2 , respectively.

The errors Δy_1 and Δy_2 result first from errors in the measurement of the wire position, and second from deviations of the wire from its position of equilibrium due to instability of the magnetic field, of the electric current, and the tension in the wire. The limitations each of these impose on the accuracy of the method are now discussed.

Consider first the uncertainty in measurement of the wire position. Combining Eqs. (4) and (5), there results

$$y_{\max} (\Delta X_f / X_f) = [\{ X_2 (X_f - X_2) + X_1 (X_f - X_1) \} / (X_2 - X_1)^2] \Delta y = a, \quad (6)$$

where Δy is the allowed typical error in the measurement of the wire position, y_{\max} is the maximum excursion of the wire at the face of the magnet and a is recognized as the aberration of the magnetic lens. Practical considerations determine the optimum choice of X_1 and X_2 , and in the case of the focusing magnets associated with The University of Michigan cyclotron,¹ the following values were employed: $X_1 = 20$ in., $X_2 = 50$ in., $X_p = 70$ in., and $X_f = 140$ in. Equation (6) now becomes $a \geq 8y$, or the allowed error

in the measurement of the wire position is an order of magnitude smaller than the aberration of the lens under test. Since the aberrations were to be less than 1 mm, the limit of the error in y is approximately 0.1 mm or 4×10^{-3} in. A description of an electrical sensor system developed to achieve the required accuracy in the wire position measurement is given in Sec. III.

Consider now the instability factors. Any deviation Δp_{eq} in the equivalent momentum p_{eq} [Eq. (3)] would deflect "ray I" to say "ray III" (Fig. 1), the distance $[F_0 F_1]$ being given by

$$[F_0 F_1] = D (\Delta p_{eq} / p_{eq}), \quad (7)$$

where D is the dispersion of the magnetic lens.¹ This deflection of the wire at the image plane would be reflected at the point X_1 , through the fixed point P_0 ,

$$y_1 = [F_0 F_1] [(X_p - X_1) / (X_f - X_p)]. \quad (8)$$

To appear stable on the wire position sensors, y_1 must be smaller than or equal to Δy [Eq. (6)]. Combining Eqs. (6) and (8) we get

$$D \frac{\Delta p_{eq}}{p_{eq}} \leq \frac{(X_f - X_p)(X_2 - X_1)^2}{(X_p - X_1)[X_1(X_f - X_1) + X_2(X_f - X_2)]} a. \quad (9)$$

Equation (9) specifies the range of values of X_1 , X_2 , and X_p given the stability $\Delta p_{eq} / p_{eq}$ of the equivalent momentum. For the magnet considered above, where $X_1 = 20$ in., $X_2 = 50$ in., $X_p = 70$ in., and $X_f = 140$ in., we obtain from Eq. (9): $D (\Delta p_{eq} / p_{eq}) = 0.18a$. Combining this with Eqs. (6) and (7) we get: $(\Delta p_{eq} / p_{eq}) = 0.18 \Delta p / p$. It can be concluded that the stability required for the equivalent momentum is about 5 times higher than that for which the magnet was designed. The equivalent momentum stability depends on the stability of three factors: B , i , and T which tightens further the stability requirement of each of these factors separately. The problem of stabilizing i and B is essentially electrical and can be accomplished in practice. The stabilization of the tension T , on the other hand, presented a mechanical problem and required the development of a special low friction pulley, which is described in Sec. IV.

Examination of Eq. (9) shows that as $(X_f - X_p)$ approaches zero the required stability $p_{eq} / \Delta p_{eq}$ approaches infinity, and that for $(X_f - X_p)$ negative, it is impossible to keep the floating wire in stable equilibrium. We conclude that in the horizontal plane, the pulley must be placed between the image plane and the magnet in order to achieve stability. In the vertical direction, on the other hand, we do not have a stable "ray" [due to the minus sign in Eq. (3) and the fact that the lens design permits double focusing of positive ions], but due to the factor mg [Eq. (1)], the wire sags somewhat, thereby introducing positive restoring forces (to deviations from equilibrium). It was

found possible, in practice, to reach stability with vertical deflections of the order of 1 mm from the median plane of the magnet.

III. THE POSITION SENSORS

The position sensors operate electrically by sensing capacitance changes between the floating wire and a pair of metal plates. A block diagram of a sensor system is given in Fig. 2.

The oscillator output of 130 kc and 10 V rms is connected to the floating wire. The "wire" (29-AWG) is free to move a few millimeters above plates consisting of two insulated copper semicircles of 2 in. in diameter. The difference of the voltages induced on each of the copper plates is amplified and fed to a phase detector triggered by the 130-kc signal from the oscillator. The output of this detector is a direct indication of the wire position.

The copper semicircles of the position sensor are mounted on a slide driven by a screw. The position of the sensor

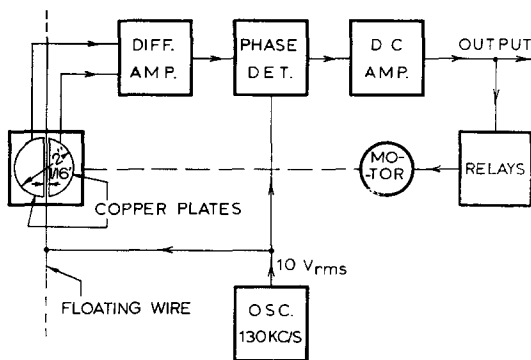


FIG. 2. Block diagram of a wire position sensor.

relative to the slide can be read by means of a vernier scale with an accuracy of $\pm 10^{-3}$ in. The screw driving the sensor is operated by a motor activated, through relays, by the amplified output of the phase detector. This closed loop system enables the sensor to follow the "floating wire" automatically with no further attention required.

Experimental testing of the sensor difference amplifier output showed that electrically the position sensitivity is about 10^{-4} in., thus, the overall sensitivity depends only on the vernier readings and is $\pm 10^{-3}$ in.

IV. THE PULLEY

As indicated in Sec. II, the stability required of the tension T in the wire is of the order of $T/\Delta T = 10^{+5}$. The tension in copper wire (29-AWG) was about 400 G, the highest tension that could safely be applied to it. Thus, the friction in the pulley must be less than 4 mg. To achieve this, a special pulley was constructed.

The pulley is made of an aluminum disk 8 in. in diameter and $\frac{1}{8}$ in. thick, two miniature ball bearings ($\frac{1}{4}$ in.) are

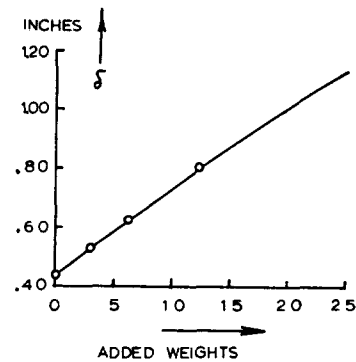


FIG. 3. Test of rotating axle bearing to freedom from friction. δ is the deflection of a point on the circumference of pulley. The sensitivity and smoothness of the curve indicate a friction smaller than 3 mg. Added weights are in milligrams.

fitted at the center and an $\frac{1}{8}$ -in.-diam axle goes through the bearings so that the pulley can revolve freely about the axle. The axle goes through two other bearings fitted into a rigid supporting frame. The bearings are New Departure miniature ball bearings (type M1624) chosen for minimum starting torque.⁵

Under operation, the axle is rotated at about 300 rpm and produces a torque on the pulley of about 0.2 g-cm. This construction was chosen in order to minimize the differential torque due to friction.

The factors governing the amount of friction are the bearings and the smoothness of the V groove in the pulley plus the characteristics of the overhanging wire. To measure the friction due to the bearing, the pulley (without the overhanging wire) was loaded by attaching weights to it and with a slight unbalance left so that the pulley acted as a pendulum with a very long period (25 sec). By adding weights of the order of milligrams and measuring the angular deflections of a point on the circumference of the pulley, curves, such as in Fig. 3, were obtained. Reproducible deflections were obtained for additions of weights as small as $\Delta T = 3$ mg, which shows that the differential friction is below the required limit of 4 mg. To find the total pulling force of the rotating axle, its speed was varied and the deflections again measured. Figure 4 gives the

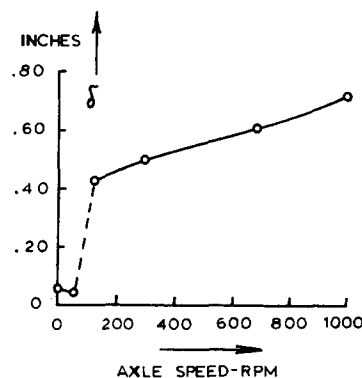
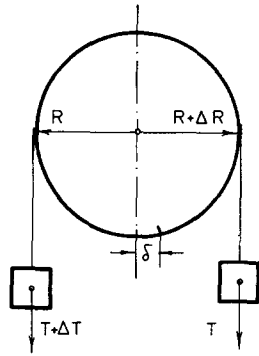


FIG. 4. Dependence of friction of rotating axle bearing on axle speed. The friction force can be deduced with the aid of curve—Fig. 3.

⁵ Since this work was completed, the design of an air supported pulley of low friction has been described by Hans Bichsel in Technical Report No. 5, Department of Physics, University of Southern California.

FIG. 5. Test setup for friction due to wire stretched over the pulley.



result of such a measurement. From Figs. 3 and 4, we conclude that the total force is about 20 mg in the region between 200 to 600 rpm. Figure 4, also shows that in this region the friction is practically independent of small variations in the rate of rotation.

To test the contribution to the friction of the wire and the V groove, the wire was stretched over the pulley and was balanced by two weights (T and $T + \Delta T$), as shown in Fig. 5. Various weights ΔT were added and the rotations of the pulley measured (the deflections δ). On plotting the graphs of ΔT vs δ hysteresis curves (with energy loss) were obtained, indicating the nonelastic properties of the stretched wire, bending and unbending as the pulley rotated.

Of the many different kinds and sizes of wires tested, the most suitable was a steel wire 6×10^{-3} in. in diameter. Figure 6 shows the hysteresis curve obtained for a copper wire, while Fig. 7 indicates no measurable hysteresis for the steel wire. Both curves show a marked "roughness" that can be explained by the roughness of the V groove on which the stretched wire rests. As indicated in Figure 5, the variations ΔR are seen to contribute directly to variations ΔT in the tension of the wire; the relative variations are $T/\Delta T = R/\Delta R$, so that from Fig. 7, we estimate the random variation to be $\Delta T \approx 30$ mg and corresponding to it, $\Delta R = R \Delta T / T = 100 \text{ mm} \times 30 \times 10^{-3} / 350 \approx 10^{-2}$ mm. A roughness of this order was difficult to eliminate in normal machining practice; but due to the excellent reproducibility of the measured points on the curve of Fig. 7, the variations in T are conservative, and should not be regarded as friction since with adequate care to reproduce the position of the pulley it is possible to reproduce T to the order of $T/\Delta T \approx 10^{+5}$.

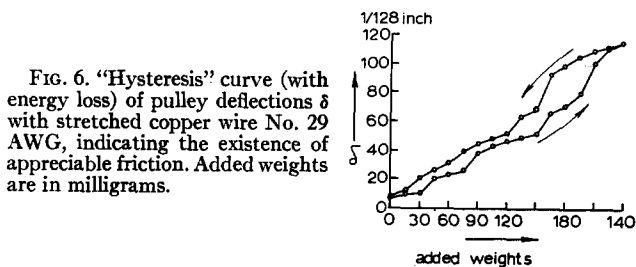
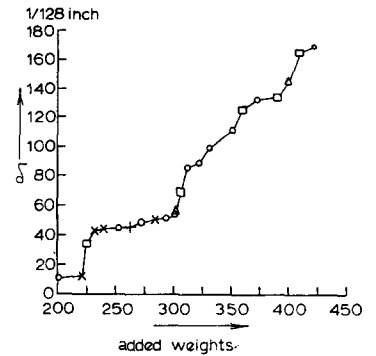


FIG. 6. "Hysteresis" curve (with energy loss) of pulley deflections δ with stretched copper wire No. 29 AWG, indicating the existence of appreciable friction. Added weights are in milligrams.

FIG. 7. Deflections of pulley with 0.006-in. steel wire. No hysteresis is detected. The excellent reproducibility (the different point markings) indicates lack of friction. The "roughness" of the curve, however, indicates imperfections in machining of pulley V groove. Added weights are in milligrams.



V. PERFORMANCE

The performance of the "floating-wire" system was tested using a magnet (1) with a radius of curvature of the optic axis of $r_0 = 200$ cm, a wedge angle $\Theta_0 = 110^\circ$, and field index $n = \frac{1}{2}$. The experimental setup is shown schematically in Fig. 1.

The pulley (P_0 or P_1) is constructed on a special motor-driven carriage and can be positioned at any point on a horizontal plane (parallel to the median plane of the magnet). The electrical sensors S_1 and S_2 move in a horizontal plane a few millimeters below the median plane. The current i in the wire is regulated to $\Delta i/i \leq 3 \times 10^{-5}$ and the magnetic field to $\Delta B/B \leq 10^{-4}$. The wire is supported on two horizontal glass rods at the faces of the magnet poles, in order to minimize the vertical sag. The friction introduced by the glass rod is minimized by vibrating the wire at about 1 kc with an audio current superimposed on the direct current i .

To test that the total friction was in fact small, the wire was allowed to reach an equilibrium position and then disturbed by rotating the pulley through a small angle. The ensuing, slowly decaying, oscillations were an indica-

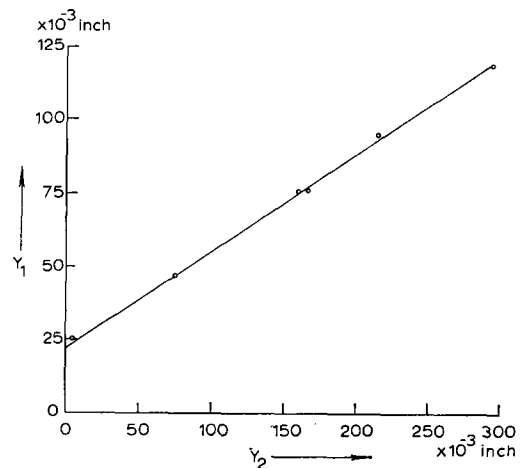


FIG. 8. Wire position sensors test. With one point fixed and the stretched wire moved about, the straight line of Y_1 vs Y_2 (position sensors readings) indicates that the total errors due to sensors and deviations of the wire from a straight line is not greater than 3×10^{-3} in.

tion that the total friction was sufficiently small. When the system was used in actual measurements, the oscillating motion of the pulley was damped with the aid of a magnet.

To test the wire position sensors, the "floating wire" was fixed at the face of the magnet and the pulley moved about. Readings of y_1 vs y_2 are plotted in Fig. 8. The straight line observed indicates the linearity of the wire and sensors, and suggests that the wire position could be determined with maximum errors of approximately 3×10^{-3} in.

As expected, the stability of the magnetic field ($\sim 10^{+4}$) was not sufficient to keep the position sensors from moving erratically around the equilibrium position. The instability could be directly measured by reading the output of the dc amplifier (Fig. 2). When used to determine the lens parameters of the magnet, this output was recorded and average readings taken, thereby reducing the uncertainty. Figure 9 gives the image distance as a function of the ray position at the face of the magnet, the zero point corresponding to the optic axis. The effects of instability are seen by the high standard deviations; the main properties of the magnet lens aberrations are, however, apparent. For an "aperture" of 2 in. on either side of the optic axis, variations of 3 in. in 144 in. are estimated. From Eq. (6) we now get the aberration:

$$a = y_{\max} (\Delta X_f / X_f) = (2 \text{ in.} \times 25.4) \times (3/144) \text{ in.} \approx 1 \text{ mm.}$$

The dispersion D and the image surface were determined by varying the "floating-wire" current and by moving the

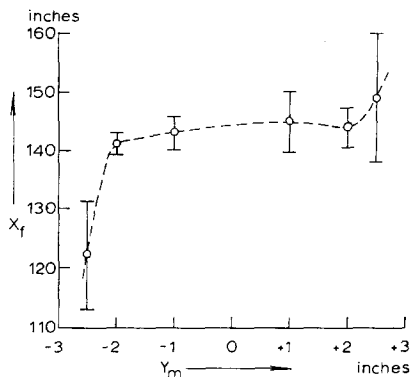


FIG. 9. The image distance (X_f) as a function of wire position (Y_{\max}) at magnet face (Fig. 1). The points and standard deviations indicated are averages of 5 measurements for each Y_{\max} . This measurement shows that the useable "aperture" of the magnet is 4 in.

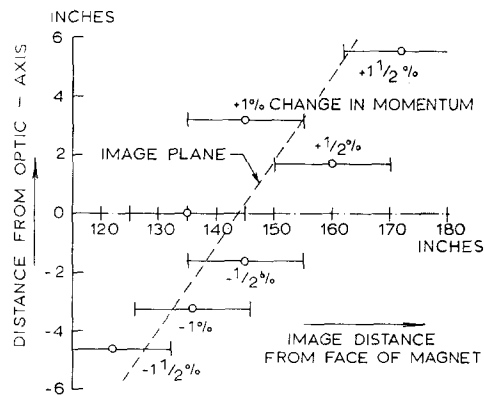


FIG. 10. Dispersion and image plane determination. No attempt was made to determine the image plane accurately and only one measurement for each momentum value was taken. A plane could be fitted with a maximum error of 10 in. in image distance. The dispersion could, however, be determined with an accuracy of $\pm 1\%$ (assuming the image distance to be accurately known).

pulley correspondingly so that the "ray" entered the first magnet face, always at the same point. The results are given in Fig. 10. A dispersion of $0.81 \text{ mm}/10^{-4}$ relative momentum change was obtained; this compares with the theoretical value (1) of 0.80.

It is concluded that the system described in this paper is capable of measuring the parameters of magnetic lens for a resolution in momentum of the order of $p/\Delta p = 10^4$. For ease and speed of measurement, it is necessary to stabilize the magnetic field to the order of $B/\Delta B = 10^6$. The system, as described, has the potential of working with less stable magnetic fields by using the electric sensors to measure the natural vibrations of the wire, thereby removing the measuring frequencies away from the range of the magnetic field variations. The development of this technique, however, was beyond the scope of this work.

ACKNOWLEDGMENTS

The author is indebted to Professor W. C. Parkinson for his guidance and advice, to Dr. K. Ramavataram and Dr. J. M. Lambert for their cooperation, and to G. Muehlehner and S. Booker for their assistance; in particular, to Muehlehner for the development of the rotating axle bearing. Appreciation is also due to K. Burch and the late R. Pittman of the cyclotron machine shop for the solution of various mechanical design problems.